Marine Pollution Bulletin 192 (2023) 115005

Contents lists available at ScienceDirect

Marine Pollution Bulletin

journal homepage: www.elsevier.com/locate/marpolbul

Impact of natural degradation of the invasive alga *Rugulopteryx okamurae* on anaerobic digestion: Heavy metal pollution and kinetic performance

David De la Lama-Calvente [a,*], María José Fernández-Rodríguez [b], José Carlos García-Gómez [c], Rafael Borja [a]

[a] Spanish Scientific Research Council (CSIC) - Instituto de la Grasa (IG), Department of Food Biotechnology, Campus Universidad Pablo de Olavide, Edificio 46. Ctra. de Utrera, km 1, 41013 Seville, Spain

[b] Department of Vegetal Biology and Ecology, Faculty of Biology, University of Seville, 41080 Seville, Spain

[c] Department of Zoology, Faculty of Biology, Universidad de Sevilla, 41080 Seville, Spain

ARTICLE INFO

Keywords:
Rugulopteryx okamurae
Invasive alien species
Ashore biomass
Heavy metal toxicity
Anaerobic digestion
Pretreatments

ABSTRACT

This study shows, for the first time, how the natural biodegradation of the Phaeophyceae *Rugulopteryx okamurae* (*R.o.*) affects its methane yield, by biochemical methane potential assays, and the methane production kinetics. Additionally, a mechanical (zeolite-assisted milling) and a thermal (120 °C, 45 min) pretreatments were assessed. The highest methane yield was obtained from the mechanically pretreated fresh ashore biomass (219 (15) NL_{CH4} kg_{VS}^{-1}), which presents the use of zeolite during milling as an economical alternative for heavy metal toxicity reduction. Moreover, no significant differences were observed between the other tests (with the exception of the lowest value obtained for the mechanically pretreated fresh *R.o.*). Low methane yields were linked to the heavy metal content. However, an increase of 28.5 % and 20.0 % in the *k* value was found for the untreated fresh *R.o.* biomass and fresh ashore biomass, respectively, when subjected to thermal pretreatment. Finally, an enhancement of 80.5 % in the maximum methane production rate was obtained for the fresh ashore biomass milled with zeolite compared to the untreated fresh ashore biomass.

1. Introduction

The invasive brown macroalga *Rugulopteryx okamurae* (*R.o.*) has expanded speedily through the Mediterranean Sea, over the last decade, uncontrolled, despite the local authorities' efforts to mitigate its ecological and economic impact (El Aamri et al., 2018; García-Gómez et al., 2021).

This invasive seaweed had shown an unprecedented competitive capacity and colonization skills in the strait of Gibraltar, where its effect is acuter due to the specific physiology of this macroalga and the occasional discharge of dissolved inorganic nitrogen into the aquatic system from terrestrial sources, among other likely factors (Mercado et al., 2022). It has provoked a severe ecological impact indicated by the immediate loss of biodiversity and the long-term changes in the structure and composition of native species (Faria et al., 2022; García-Gómez et al., 2020). The algae have colonised >90 % of the solid substrates, up to 20 m deep, in the Strait Natural Park sea-coast, and although at deeper cotes its presence is diminished, it is still high (30–40 %) (MITECO, 2022). Moreover, the generated biomass loosed and reached the beaches causing an impact on sea-dependant anthropogenic activities which costed 1.2 million euros in the 2019 season due to beach-waste management and the lost in the fishery sector (MITECO, 2022).

R.o. has become a good study-case for the management of both invasive alien macroalgae and "algae-tides" in the coast. Just in the 2019 season, ten thousand tonnes of biomass between January and September were removed from only 5 coast-towns in the south of Spain with an overall cost of 400,000 euros (MITECO, 2022). Eradication of invasive alien seaweed although it is the main objective of local authorities affected by their presence it is not yet effective (MITECO, 2022). Most pilot assays have been carried out by removing the algae manually, which has an extreme cost in time and human resources (MITECO, 2022). Thus, the control of the expansion is nowadays a more feasible enterprise. In this sense, several studies have been focused on this task, with a certain degree of success, by manually removing the algae after salt treatments, by asphyxiation methods or even using chemical biocides (Anderson, 2005; Madl and Yip-Wong, 2005; Williams and

Abbreviations: FAR, fresh ashore *Rugulopteryx okamurae*; TF, Transference function.

* Corresponding author.
E-mail address: dlama@ig.csic.es (D. De la Lama-Calvente).

https://doi.org/10.1016/j.marpolbul.2023.115005
Received 22 December 2022; Received in revised form 25 April 2023; Accepted 28 April 2023
Available online 9 May 2023

Schroeder, 2004). However, very little success has been reached in sea open water cases. Thus, most of the scientific and political efforts have been centred on the valorisation of the biomass.

Brown seaweeds are well known in the scientific literature. They have been studied as a source of food-additives (e.g. alginates, lipids, etc.), of bioactive compounds or for the production of bioplastics, among others uses (Casal-Porras et al., 2021; Puri et al., 2022; Santana et al., 2022). However, its use as fuel has centred the focus of the scientific community. The use of macroalgae biomass as a substrate for the production of bioethanol, biohydrogen or biomethane has been widely studied and it has been also applied industrially, although in relatively small scales (Leong and Chang, 2022; Pardilhó et al., 2022; Zollmann et al., 2019).

Among the technologies used for the conversion of seaweed into fuel, anaerobic digestion (AD) for the production of biomethane is presented as one of the most promising technologies, mainly due to: i) the technology is well known and it has been used at industrial scale; ii) it fits all the requirements for a circular economy model; iii) it can be introduced successfully into a biorefinery concept; iv) the digestate can be used as biofertilizers (Leong and Chang, 2022; Thompson et al., 2019).

Nevertheless, the AD of seaweed, although widely studied, still presents several drawbacks that need more attention prior to its scaled-up: i) low and variable C/N ratio (6–20); ii) high presence of non-biodegradable compounds (e.g. cell-wall components); iii) seasonal variation; iv) heavy metal and salt toxicity, etc. (Jard et al., 2013; Nielsen et al., 2020; Saratale et al., 2018; Zheng et al., 2022). Literature shows several attempts to overtake these issues, mostly by anaerobic co-digestion (AcoD) or by the use of different pretreatments, being thermal and chemical treatments the most investigated (Saratale et al., 2018; Thompson et al., 2019).

Nevertheless, although the seasonal and spatial variation effects on methane yield of several macroalgae have been previously reported, to the best of our knowledge the impact on the AD performance of the natural degradation of marine seaweed from its natural location to the naturally fermented biomass formed at the ashore-beach has not been yet assessed. Therefore, this research aims to investigate the impact of the natural degradation of the invasive brown macroalgae *Rugulopteryx okamurae* on the methane yield. Two different stages (i.e. immediately once it reached the beach and after 5 months left ashore) were compared with its natural form (i.e. offshore deep waters). Moreover, the effect of zeolite-assisted milling and thermal pretreatments (120 °C, 45 min) on the methane potential of the different biomass was assayed as well. Furthermore, a comprehensive heavy metal analysis of the biomass and its effect on the AD process were also evaluated. Finally, kinetic modelling of the tests has been assessed.

2. Material and methods

2.1. Analytical methods

The anaerobic feed (assayed biomasses before and after pretreatment) were analysed prior the biochemical methane potential (BMP) set-up (Table 1) and also the inoculum sludge. Moreover, the resultant digestates of the AD process were also reviewed and analysed (Table 2). For the analysis of soluble parameters, samples were previously centrifugated (Eppendorf, 9000 ×*g*, 10 min) and filtrated (Albet, 47 mm glass fiber filter). The different solid fractions (i.e. total solids (TS), volatile solids (VS) and mineral solids (MS)) were obtained by following the standard method 2540B & 2540E (APHA, 2017). Total ammonia nitrogen (TAN) was performed by distillation and titration following the standard method 4500-NH_3 (APHA, 2017). Total chemical oxygen demand (COD_{total}) and soluble chemical oxygen demand (COD_{sol}) were carried out as described by Raposo et al. (2008) and the standard method 5220D (APHA, 2017), respectively. pH and total alkalinity (TA) were performed by using a pH meter model Crison 20 basic, and TA was analysed by titration to pH 4.3 as described in the standard method 2320B (APHA, 2017). Elemental analysis of the lyophilized biomasses was performed by a LECO TruSpec® Micro Elemental Analyzer (Leco Corporation, USA). Trace elements determination was carried out by digesting the samples as described in the U.S. EPA 3051A method (800 W, 175 °C, 8:00 min ramp, 4:30 min hold) (USEPA, 2007) by using a Mars Xtraction microwave (CEM, USA). The digested solution was then diluted when necessary and analysed by Inductively Coupled Plasma Mass Spectrometry (ICP-MS, AGILENT 7800, Spain). Finally, the microstructural characterization was assessed by scanning electron microscopy (SEM) using a FEI Teneo instrument in transmission mode.

2.2. Anaerobic sludge

The used anaerobic sludge for all the BMP assays was selected due to its high methanogenic activity, as it had been several times confirmed by the research group and by using positive controls along with the experiments. Immediately after its collection from a nearby brewery wastewater anaerobic treatment plant, the sludge was placed in a water bath at 35 (2) °C for 36 h before its use in order to lessen the endogenous methane production.

The main physicochemical parameters of the selected sludge were as follow: TS, 56.0 (0.7) g kg^{-1}; VS, 37.5 (0.5) g kg^{-1}; COD_{total}, 42 (4) g O_2 kg^{-1}; pH, 7.59 and TA, 3600 (200) mg $CaCO_3$ L^{-1}.

2.3. Seaweed biomass

The invasive *R.o.* was collected by the Laboratory of Marine Biology

Table 1
Main physicochemical parameters of the macroalga *Rugulopteryx okamurae* (*R.o.*) collected at different degradation times, before and after the applied pretreatments.

Parameter[a]	Fresh *R.o.*			Fresh ashore *R.o.*			Dried ashore *R.o.*		
	Control	Thermal pret.	Zeolite pret.	Control	Thermal pret.	Zeolite pret.	Control	Thermal pret.	Zeolite pret.
TS (g kg^{-1})	226 (6)^{1}	288 (1)^{2}	219 (2)^{1}	219 (4)^{1}	216.8 (0.8)^{1}	183 (3)^{3}	752 (2)^{4}	925 (3)^{5}	718 (23)^{4}
VS (g kg^{-1})	159 (5)^{1}	205 (3)^{2}	146 (2)^{3}	169 (4)^{1}	163 (3)^{1}	129 (2)^{4}	524 (4)^{5}	646 (8)^{6}	501 (34)^{5}
VS/TS ratio	0.71	0.71	0.67	0.77	0.75	0.71	0.70	0.70	0.70
MS (g kg^{-1})	66.4 (0.9)^{1}	83 (1)^{2}	73.4 (0.4)^{3}	50.0 (0.2)^{4}	54 (2)^{5}	53.6 (0.6)^{5}	228 (3)^{6}	278 (4)^{7}	220 (10)^{6}
CODtotal (g O_2 kg^{-1})	228 (5)^{1}	237 (2)^{1}	206 (7)^{2}	238 (9)^{1}	230 (20)^{1}	159 (1)^{3}	770 (30)^{4}	720 (6)^{5}	710 (20)^{5}
C (%)[b]	33.1 (0.9)^{1}	35.6 (0.9)^{2}	32.7 (0.5)^{1}	37 (2)^{3}	37 (2)^{3}	32.8 (0.2)^{1}	32 (1)^{1}	32.5 (0.5)^{1}	32.6 (0.6)^{1}
N (%)[b]	2.707 (0.009)^{1}	2.87 (0.08)^{2}	2.63 (0.08)^{1}	2.1 (0.1)^{3}	1.6 (0.3)^{3}	1.7 (0.2)^{3}	3.0 (0.2)^{2}	3.0 (0.1)^{2}	2.69 (0.06)^{1}
H (%)[b]	4.7 (0.2)^{1}	4.9 (0.2)^{1}	4.6 (0.2)^{1}	4.9 (0.3)^{1}	5.1 (0.2)^{1}	4.5 (0.2)^{1}	4.7 (0.3)^{1}	4.5 (0.3)^{1}	4.8 (0.1)^{1}
O (%)[b]	30 (1)^{1}	28 (1)^{2}	26.6 (0.7)^{2}	34 (2)^{3}	32 (2)^{1}	31.7 (0.4)^{1}	30 (1)^{1}	30.0 (0.9)^{1}	29.7 (0.6)^{1}
C/N ratio	12.2	12.4	12.4	17.6	22.6	19.2	10.9	10.7	12.1
$BMP_{th,COD}$ (NL_{CH4} kg_{VS}^{-1})	500	403	494	493	498	431	511	390	496
$BMP_{th,CHON}$ (NL_{CH4} kg_{VS}^{-1})	448	495	489	451	512	489	447	436	456

[a] Values represent mean (standard deviation). Different superscripted numbers in the same row indicate values are significantly different (α = 0.05).
[b] Results based on dry matter.

Table 2
Main physicochemical parameters of the digestates obtained after BMP tests of different *Rugulopteryx okamurae* (*R.o.*) biomasses.

Parameter[a]	Fresh *R.o.*			Fresh ashore *R.o.*			Dried ashore *R.o.*		
	Control	Thermal pret.	Zeolite pret.	Control	Thermal pret.	Zeolite pret.	Control	Thermal pret.	Zeolite pret.
pH	7.8 (0.2)^{1}	7.9 (0.1)^{1}	7.8 (0.2)^{1}	7.8 (0.1)^{1}	7.90 (0.03)^{1}	8.0 (0.1)^{1}	8.1 (0.1)^{1}	7.9 (0.2)^{1}	7.87 (0.04)^{1}
TA (mg $CaCO_3$ L^{-1})	4500 (200)^{1}	4230 (50)^{1}	4000 (400)^{1}	4200 (100)^{1}	4100 (200)^{1}	4800 (300)^{1}	4500 (200)^{1}	4400 (500)^{1}	5000 (500)^{2}
Conductivity (mS cm^{-1})	9.6 (0.5)^{1}	8.5 (0.7)^{1}	9 (1)^{1}	8.25 (0.05)^{2}	8.4 (0.4)^{2}	10.1 (0.2)^{1}	9.9 (0.6)^{1}	9.4 (0.7)^{1}	10.1 (0.5)^{1}
TS (g kg^{-1})	29.9 (0.4)^{1}	29.5 (0.4)^{2}	31.8 (0.5)^{3}	29.1 (0.5)^{2}	29.4 (0.7)^{2}	31 (1)^{3}	35.0 (0.6)^{4}	33 (1)^{5}	31 (1)^{3}
VS (g kg^{-1})	19.1 (0.3)^{1}	18.7 (0.4)^{1}	19.9 (0.4)^{2}	18.6 (0.4)^{1}	18.9 (0.7)^{1}	19 (1)^{1}	22.4 (0.4)^{3}	21 (1)^{4}	19 (1)^{1}
MS (g kg^{-1})	10.8 (0.2)^{1}	10.9 (0.2)^{1}	11.8 (0.3)^{2}	10.5 (0.3)^{3}	10.5 (0.1)^{3}	12.2 (0.1)^{4}	12.6 (0.4)^{5}	12.1 (0.3)^{4}	12.5 (0.1)^{5}
VS/TS ratio	0.64	0.63	0.63	0.64	0.64	0.61	0.64	0.63	0.60
CODs (g O_2 kg^{-1})	410 (30)^{1}	290 (30)^{2}	320 (20)^{2}	200 (20)^{3}	170 (20)^{4}	170 (10)^{4}	60 (20)^{5}	130 (20)^{6}	270 (70)^{2}
TAN (mg NH_3-N kg^{-1})	800 (30)^{1}	730 (30)^{2}	820 (60)^{1}	770 (20)^{1}	670 (50)^{3}	880 (40)^{4}	680 (50)^{3}	620 (50)^{5}	710 (40)^{3}
BMP_{exp} (NL_{CH4} kg_{VS}^{-1})	93 (4)^{1}	150 (30)^{1}	65 (3)^{2}	160 (20)^{1}	130 (50)^{1}	220 (20)^{3}	100 (10)^{1}	120 (30)^{1}	100 (30)^{1}
$Biodegradability_{COD}$	19 %	38 %	13 %	33 %	27 %	51 %	20 %	31 %	22 %
$Biodegradability_{CHON}$	21 %	31 %	13 %	36 %	26 %	50 %	23 %	28 %	23 %

[a] Values represent mean (standard deviation). Different superscripted numbers in the same row indicate values are significantly different (α = 0.05).

of the University of Seville from three different spots along the Algeciras coast: i) Fresh *R.o.* (**FR**) from off-shore deep waters in its natural stage; ii) Fresh Ashore *R.o.* (**FAR**), immediately collected once the biomass reaches the beach; iii) Dried Ashore *R.o.* (**DAR**), collected from the beach 5 months since it arrives.

FR and **FAR** samples were washed with sea water in-situ in order to eliminate as much as possible any debris and stored at −20 °C until further use. **DAR** samples were not washed, in order to keep their dryness, and it was stored at −20 °C as well.

Before any further use, the samples were unfrozen at 4 °C for 2 h and any observable debris in plain sight was left aside. It was observed that **DAR** samples were difficult to clean and it was not possible to guarantee that only the seaweed *R.o.* was present in the sample. However, the experiment was continued as the objective of the research was to assess the feasibility of the AD over a natural degradation process, which in this case, involved the mixture of the algae with coast biota. Nevertheless, it was confirmed that **DAR** samples were composed mainly of *R.o.* in an 80–90 % degree.

2.4. Zeolite

The zeolite used during the study was from natural sources and donated by the Laboratory of Zeolites of the University of Havana, Cuba. The zeolite consists in a mixture of clinoptilolite (70 %), mordenite (5 %), anorthite (15 %), and quartz (10 %). The chemical composition of the material in oxide form was SiO_2, 67 %; Al_2O_3, 11 %; CaO, 4 %; Na_2O, 2 %; K_2O, 1 %; MgO, 0.7 %; and Fe_2O_3, 2 % with an average moisture content of 12 %. The zeolite was also grounded and sieved in order to obtain a 30–90 μm particle size.

2.5. Experimental set-up

2.5.1. Pretreatments

All samples were subjected to a milling process by a blade blender. The process was performed for 30 s for each 10 g batch of biomass. This guarantee an average final particle size of 1–10 mm. Based on previously reported research (De la Lama-Calvente et al., 2023), two pretreatments that provided the best methane yield results on a previous collected **FR** were selected for this research: i) The zeolite-assisted mechanical pretreatment, carried out by adding a 5 % (VS basis) of zeolite to the biomass prior its milling; ii) The thermal pretreatment, carried out at 120 °C during 45 min.

The samples were labeled as follows: **FRC:** untreated Fresh *R.o.* as Control; **FRT:** Fresh *R.o.* Thermally pretreated; **FRZ:** Fresh *R.o.* milled with Zeolite; **FARC:** untreated Fresh Ashore *R.o.* as Control; **FART:** Fresh Ashore *R.o.* Thermally Pretreated; **FARZ:** Fresh Ashore *R.o.* milled with Zeolite; **DARC:** untreated Dried *R.o.* as Control; **DART:** Dried Ashore *R.o.* Thermally Pretreated and **DARZ:** Dried Ashore *R.o.* milled with Zeolite.

2.5.2. Biochemical methane potential (BMP) test

BMP assays were performed as described by Holliger et al. (2016), and each test was executed in triplicates. The selected temperature of the experiment was within the mesophilic range (35 ± 1 °C) and it was maintained constant throughout the experiment. The inoculum to substrate ratio (ISR) based on VS was maintained at 2 in each reactor. 250 mL reactors were filled with the selected substrate and the inoculum so the total final concentration was 24 g VS L^{-1}. Additionally, a 0.1 % (*v*/*v*) micronutrient solution as described in Fernández-Rodríguez et al. (2020) and distilled water up to a working volume of 250 mL was added to each test. The head space was maintained at minimum and it count for less of 10 % of the total volume. Once the reactors were filled with the mixture, they were placed into a water bath and flushed with nitrogen gas in order to remove the oxygen and thus guarantee the anaerobic conditions.

Three blanks, consisting of a mixture of inoculum, water and micronutrient solution, were prepared, and, as positive control, microcrystalline cellulose (Avicel® PH-101, Fluka) was used as substrate.

The produced methane was measured volumetrically by passing the generated biogas through a 2–3 N NaOH solution as supported by Casallas-Ojeda et al. (2022) and as had been widely reported in the literature. Once the accumulated volume of methane was <1 % for three days in a row, the experiment was considered completed, this period was c.a. 31 d across the board. Then, the endogenous methane production from the blanks was subtracted to the methane yield of each assay and the results were normalized to standard temperature and pressure conditions (273.15 K and 101.33 kPa).

2.6. Data analysis

2.6.1. Statistical analysis

Analysis and experiments were at least carried out in triplicates and values are given by means (standard deviation). Where corresponded, a two-tale Student's *t*-test and the one-way analysis of variance (ANOVA) were carried out. For the purposes of data discussion, a confidence level of $\alpha = 0.05$ was accepted as not statistically significant.

2.6.2. Biodegradability

The biodegradability of each substrate was calculated by both the COD_{total} and the elemental composition (CHON) analysis as proposed by Nielfa et al. (2015). Biodegradability results are displayed in Table 2 while the theoretical methane yield is shown in Table 1.

2.6.3. Kinetic models

The process kinetics of the different substrates were studied by applying different models were considered. Two different models were used, i.e.: First-order; Transference function (TF). Further details about equations are described widely in the literature, however, they are also shown in the Supplementary Material.

2.6.4. Preliminary energy and economic assessment

The authors of this paper acknowledge the difficulties to perform a comprehensive economic evaluation with data provided by a lab-scale batch system, thus, this study aims to compare only the differences between treatments rather than assess an overview of a hypothetic industrial scale.

Moreover, in order to simplify the study, several assumptions were made: i) only the energy consumption of milling and thermal treatment were considered; ii) the heat to keep the temperature of the AD process of *R.o.* biomass at 35 °C was recovered after thermal treatment using heat exchangers with an efficiency (η) of 85 % (Ding et al., 2020); iii) the initial temperature of *R.o.* before the treatment was stablished at 25 °C; iv) the specific heat capacity of *R.o.* was assumed to be similar to water, i.e. 4.18 kJ kg^{-1} $°C^{-1}$; v) the energy consumed during the complete thermal treatment was considered equal to the energy consumption of the start-up multiplied by the treatment time; vi) the energy price has been set up as the average industrial retail price of electricity in the USA by May 2022, which was 8.96 cents $ kWh^{-1} (EIA, 2022) and also as the average price in the second semester of 2021 in the EU, which was 144.5 cents € kWh^{-1} (EC, 2022); vii) zeolite cost has been established at 50 to 300 $/ton as reported by the United States Geological Service (USGS, 2022). Further details about the used equations and the results obtained in this preliminary energy and economic assessment are included in the Supplementary Material.

3. Results and discussion

3.1. Physicochemical and microstructural characterization

3.1.1. Physicochemical analysis

Table 1 shows the principal physicochemical parameters of the seaweed *R.o.* collected at different stages and with or without pretreatments. As can be seen, although there were no significant differences between **FRC** and **FARC** in terms of TS and VS (219 (4)–226 (6) and 159 (5)–169 (4), respectively), the dried biomass (**DARC**) showed a much higher content of TS (752 (2)), which was due to the biomass being sun-dried at open air left ashore for 5 months. However, since the ratio VS/TS remains quite similar regardless the sample (0.70–0.77), it could be concluded that there is not a significant decrease in the organic matter content, although the type of compounds was expected to differ. This was also confirmed by comparing the COD_{total} results in terms of TS. The fresher samples (**FRC** and **FARC**) presented a moisture content similar to those reported in the literature. Jard et al. (2013) reported water contents, of 10 fresh seaweed species, ranging from 94.5 % to 81.5 %. Thompson et al. (2019) also pointed out that brown seaweeds presents a moisture content from 70 % to 90 %. However, the naturally dried biomass (**DARC**) showed a moisture content higher than that expected for a sun-dried sample as reported by several authors (Hassaan et al., 2021; El Nemr et al., 2021; Suwati et al., 2021). This higher moisture content was possibly due to the composting structure of the biomass which presented a drier upper-layer acting as a cover and, hence, maintaining a more humid biomass underneath in contrast with the sun-dried biomasses evaluated in lab conditions where the algae was placed evenly through the surface guaranteeing the same dryness along the samples. More drastic differences were observed between C/N ratios, ranging from 10.9 to 17.6. Olivera et al. (2014) reported that the drying process of the red macroalgae *Gracilaria vermiculophylla* slightly increased the total Kjeldahl nitrogen as well as the protein content of the biomass, which could explain the lower C/N ratio of **DARC** (10.9). This could be also due to the composting process over the algae biomass. Several authors have reported that the C/N ratio of the biomass subjected to a compost process could decay from 20–40 to 7 (Michalak et al., 2017). However, the differences between **FARC** (17.6) and **FRC** (12.2) in terms of the C/N ratio must be regarded to the evolution of the main biochemical compounds (i.e. carbohydrates, lipids and proteins) of the macroalgae through its life-cycle as also supported by several reports (Jard et al., 2013; Thompson et al., 2019).

Thermal pretreatment strongly reduced the moisture content of the **DAR** sample, although this effect was less acute with the **FR** biomass, and insignificant for the **FAR** sample. This could be due to the non-structural water (i.e. water as moisture in the biomass surface) being evaporated easier during the thermal treatment. In the **DAR** case, water on the surface was mainly the only water source in the sample, while **FR** and **FAR** presented a higher inner-cell water proportion. Moreover, this treatment increased significantly the C/N ratio of **FAR** (from 17.6 to 22.6), while not affecting it for **DAR** or **FR** (10.9–10.7 and 12.2–12.4, respectively). Brown et al. (2020) observed that the hydrothermal carbonisation treatment at 150 °C of both macroalgae *Saccharina latissima* and *Fucus serratus* reduced the C/N ratio. However, this same study reported that at higher temperatures the C/N ratio increased when compared with the untreated sample. This is due to the increase in fixed carbon with the temperature, while N increased at 150 °C but not at the higher selected ranges. In the present study, while the total C remains unchanged, N is reduced, similarly as it happened during sun-drying (Olivera et al., 2014).

Regarding the zeolite-assisted milling treatment, it slightly increased the moisture content of **FAR**, while not affecting significantly the other two substrates. This is in accordance with the thermal treatment result, being **FAR** the biomass with the lowest content in surface-water. Zeolite could act as a hygroscopic material and absorb some ambient moisture during the process. This absorbed water content must be minor, as it wasn't observed in other samples, however, having the **FAR** sample such a low surface-water, the absorption process could had been leveraged. Nevertheless, the C/N ratio of **FAR** and **DAR** increased, while it remained the same for **FR**, which could be related to a higher loss on nitrogen components due to seasonal variations.

The theoretical methane yield of each tested biomass was also calculated, with values ranging from 390 to 511 NL_{CH4} kg_{VS}^{-1} (COD_{total} based) and from 436 to 512 NL_{CH4} kg_{VS}^{-1} (CHON based). These values were similar to those reported in the literature within the range of 400 to 1000 NL_{CH4} kg_{VS}^{-1} (Darko et al., 2022). Based on all the above, a good AD performance could be expected, since the VS/TS ratio was within the optimum range (>0.5), and the C/N ratio, although low, was within the range of other reported successful assays (6–20) (Jard et al., 2013; Wang et al., 2016).

3.1.2. Heavy metals

Table 3 shows the elemental analysis of the raw algae collected at different stages. Generally, the main differences between the samples assayed in the present work could be related to their collected points and life cycle stage. Similar differences were reported for the brown macroalgae *Padina vickersiae* when collected from different points along the shores of Havana City, Cuba (Ramírez et al., 1989). More recently, Gao et al. (2022) observed differences on the heavy metal contents within the food web due to seasonal variations within a year. These changes along the life cycle could be related to the different needs to carry out specific bioactivities or the bioaccumulation capacity of the seaweed in equilibrium with the seawater salts concentrations, as the physicochemical variations of the water (e.g. pH, turbidity, etc.) affects the synthesis of different macroalgae compounds (Júnior et al., 1991). Following this, Michalak et al. (2017) assessed the viability of composting a green and red seaweed consortium that reached the coast of the Baltic Sea. The elemental analysis of the biomass before and after the compost treatment showed an increase in macro and micronutrients such as Ca, Cu, Fe and P, as well as in other toxic heavy metals. In the present study, although most of the analysed metals increased in the drier sample (e.g. B, Na, Mg, Ni), a significant reduction of others was observed (e.g. Cu, Hg). Hence, the differences related to the **DARC**

Table 3
Elemental and metal compositions of different biomasses of *Rugulopteryx okamurae* (*R.o.*) tested.

Parameter[a]	Natural *R. o.*	Fresh ashore *R. o.*	Dried ashore *R. o.*	Natural *R. o.*[b]
B (ppm)	600 (20)	460 (60)	800 (100)	nd[c]
Na (g kg^{-1})	43 (5)	44.7 (0.7)	130 (20)	73.7 (0.6)
Mg (g kg^{-1})	10 (1)	10.4 (0.9)	31 (6)	13.2 (0.4)
Al (g kg^{-1})	2.0 (0.3)	1.0 (0.1)	1.4 (0.1)	1.1 (0.6)
P (g kg^{-1})	1.37 (0.03)	0.88 (0.02)	1.76 (0.02)	1.3 (0.1)
K (g kg^{-1})	80 (10)	49 (4)	120 (20)	nd[c]
Ca (g kg^{-1})	89 (3)	48 (8)	100 (20)	29.2 (0.5)
Cr (ppm)	80 (50)	40 (20)	99 (5)	6.5 (0.2)
Mn (ppm)	50 (6)	100 (10)	70 (10)	42 (4)
Fe (g kg^{-1})	2.4 (0.5)	2.0 (0.3)	3.8 (0.7)	2.0 (0.2)
Co (ppm)	1.00 (0.01)	1.4 (0.4)	2,2 (0,3)	1.7 (0.5)
Ni (ppm)	32 (2)	60 (40)	100 (20)	20.9 (0.1)
Cu (ppm)	70 (30)	31.3 (0.8)	24.6 (0.6)	6.1 (0.1)
Zn (ppm)	140 (20)	100 (10)	110 (9)	18.9 (0.1)
As (ppm)	27 (4)	17 (2)	54 (7)	41.6 (0.6)
Mo (ppb)	4060 (10)	6000 (2000)	4100 (900)	570 (20)
Cd (ppb)	660 (6)	130 (10)	940 (70)	240 (20)
Sn (ppb)	2000 (300)	200 (20)	1800 (400)	50 (20)
Ba (ppm)	490 (80)	290 (40)	360 (40)	19.6 (0.2)
Hg (ppm)	31.4 (0.4)	23 (2)	21 (2)	2.3 (0.7)
Pb (ppm)	14 (2)	5 (2)	14 (3)	1.9 (0.1)

[a] Values represent mean (standard error). Based on dry matter.
[b] De la Lama-Calvente et al., 2023.
[c] Not determined.

biomass in comparison with fresher biomasses, could be explained in terms of compost decomposition, while losses due to lixiviation into the land cannot be discharged.

However, and more importantly, a high content of toxic heavy metals was observed regardless the biomass. For that reason, the elemental analysis of a previous sample similar to **FRC** but harvested a year earlier is shown along with the new samples in the Table 3 in order to facilitate the discussion. While there were no significant differences when some essential minerals were compared (i.e. Na, Mg, Al, Mn, Fe and Co), a significant increase of others were found in the latter samples. For example, Mo concentration in the new sample was 4060 (10) ppb while its concentration in the previous samples was only 570 (20), almost 10 times lower. Similar results were found for Cu, Zn, Cr, Cd, Sn, Ba, Hg and Pb. Macroalgae have been studied for its capacity to remove contaminants from saline waters. In a recent study, Fabre et al. (2021) reported that the green macroalgae *Ulva intestinalis* had great affinity to mercury showing an uptake capacity of 1888 ppm and a removing ability of 99.9 % to 98.2 % when the Hg concentration in the saline waters ranged from 50 to 500 μg dm^{-3}, respectively. Chynoweth (1981) showed that lots of *Macrocystis pyrifera* obtained in summer presented lower levels of N and P when compared with the lots harvested during the winter months. These results are in agreement with others found in the literature, for example, when different lots of the brown macroalgae *Laminaria digitata* were analysed, results showed that although most of the metals were present in similar concentrations (Na, K, Ca, S, Sr, P, Fe, Zn, …), some toxic heavy metals were found in concentrations four times (Cr and PB) and twenty-eight times (Ni) higher (Alvarado-Morales et al., 2015).

Nevertheless, these results were of main concern. Although it is well known that traces of some minerals are beneficial to the AD process, these elements at certain concentrations and oxidation states could potentially inhibit the performance (Guo et al., 2019). Zheng et al. (2022) assessed the toxicity of Cu, Zn, Cd, As and Pb during the AD of animal manure. This study showed that Cu is unstable under oxidising conditions and it could provoke long-term toxicity, while Zn and Cd presented a higher bioavailability and, hence, toxicity. Pb, on the other side, was found in the stable fraction, showing the lowest toxicity since it did not enter the food chain. Additionally, the AD process could increase the heavy metal concentration of the biomass due to the decomposition of the organic fraction (Zheng et al., 2022). Similarly, Alrawashdeh et al. (2020) reported that the toxicity of the assessed heavy metals during the AD of olive mill waste could be arranged in the following increasing order: Cu > Ni > Pb > Cr > Zn > Fe. Although, further investigation needs to be carried out in order to fully understand the toxicity pathways of most of the elements, some insights have been already reported. Guo et al. (2019) reported that Cu, Ni, Cd and Zn were toxic to methanogenic archaea, while Cu and Ni also inhibit the enzymatic activity of cellulase.

3.1.3. Structure analysis

Fig. 1 shows the SEM images of the fresh ashore macroalgae (**FAR**) before and after each treatment. Images showed a smoother surface for the untreated biomass (Fig. 1a) along with typical folds observed in previous studies on this and other brown algae (De la Lama-Calvente et al., 2023; Bogolitsyn et al., 2020). However, after the thermal or the zeolite-assisted milling pretreatment, the biomass surface became more wrinkled and micro-pores are exhibited along the surface. It was also observed that these differences were acuter after the thermal pretreatment (Fig. 1b) than after the use of zeolite during the milling step (Fig. 1c). These findings were in accordance with previous reported results suggesting that these changes could improve the contact between the substrate and the microbial communities during the AD process, and, more specifically, allow for more frequent interaction between the organic matter of the substrate and the microbial enzyme glucoamylase (De la Lama-Calvente et al., 2023; Ding et al., 2020).

3.2. Biochemical methane potential performance

Fig. 2 shows the methane yield curves of the different assays carried out versus time, while the specific accumulative methane yields are included in Table 2, along with other physicochemical parameters of the digestates. As it can be seen, digestates presented pH (7.8 (0.2)–8.1 (0.1)), TA (4000 (400)–5000 (500) mg $CaCO_3$ L^{-1}) and TAN (620 (50)–880 (40) mg NH_3-N kg^{-1}) values within the optimum range for a stable AD process (Holliger et al., 2016) regardless the location and the pretreatment of the biomass. These results support the idea of an AD process not inhibited due to the accumulation of short-chain fatty acids, which inhibits the acetogenic and methanogenic activity and would be translated into a lower pH and an unbalanced TA (Choi et al., 2023), or by the production of ammonia, as being the TAN below the toxic limit of free ammonia established at 2000 mg L^{-1} (Yenigün and Demirel, 2013).

Methane yield did not show significant differences between most of the scenarios assessed, with values ranging from 93 (4) to 160 (20) NL_{CH4} kg_{VS}^{-1}. Only two experiments showed statistically different yields, the tests **FARZ** (220 (20) NL_{CH4} kg_{VS}^{-1}) and **FRZ** (65 (5) NL_{CH4} kg_{VS}^{-1}). These results are comparable with others report in the literature. For example, Ayala-Mercado et al. (2021) reported no significant differences in the methane yield of pelagic *Sargassum* when subjected to steam explosion in comparison with the extrusion pretreatment, reaching yields of 114 (4) and 108 (6) NL_{CH4} kg_{VS}^{-1}, respectively. It is also worth noticing the differences obtained in the methane yield of the natural fresh *R.o.* when compared with previously reported results (De la Lama-Calvente et al., 2023). Differences in methane yield were expected as the algae were collected at different periods of time, which is in accordance with other reported results. Jard et al. (2013), showed differences of almost 25 % in the methane yield of the macroalgae *Saccharina latissima* when collected in May or in June of the same year. In our study, the difference is up to 50 % less for the untreated algae, 40 % less for the thermally treated algae and >70 % less for the *R.o.* milled with zeolite. Moreover, while the zeolite-assisted milling process enhanced greatly the methane yield in previous studies, it showed a significant negative effect on this new harvested batch (De la Lama-Calvente et al., 2023). Montingelli et al. (2016) reported that the mechanical pretreatment effect was highly dependent on the harvesting period, thus, the highest methane yield obtained in November (ISR = 3; beating time = 5 min) was 59 and 43 % higher than the highest yields achieved in May (ISR = 1.2; beating

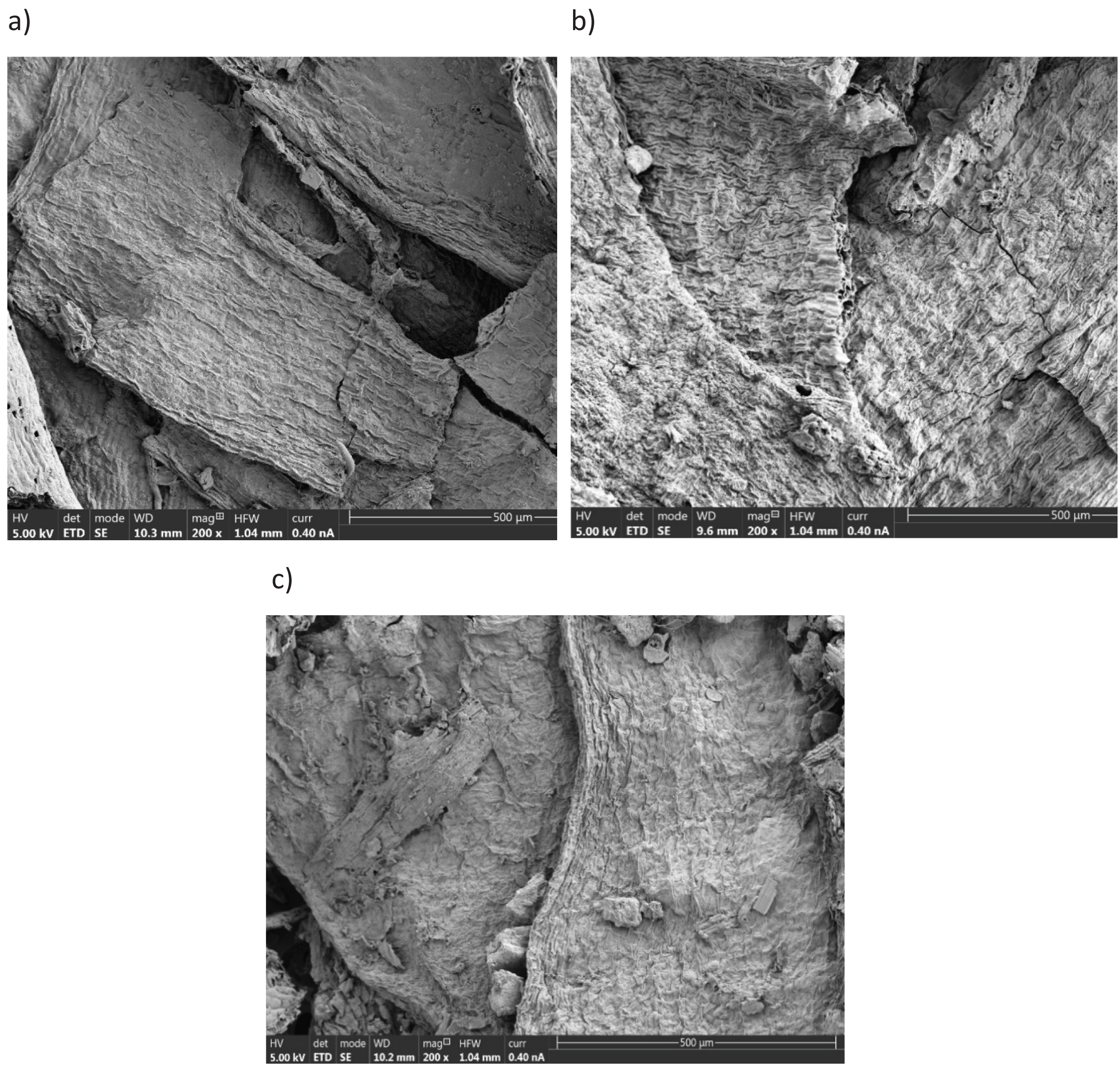

Fig. 1. SEM images of a) fresh ashore *Rugulopteryx okamurae* (*R.o.*) untreated (**FARC**), b) fresh ashore *R.o.* thermally treated (**FART**) and c) fresh ashore *R.o.* zeolite-assisted during milling step (**FARZ**).

time = 15 min) and March (ISR = 1.2; beating time = 15 min), respectively. However, in the present study, these great differences could not be related to only seasonal variations in terms of carbohydrates, lipids or sugar concentration (Adams et al., 2011; Chynoweth, 1981). As discussed above, heavy metal toxicity seems to play an essential role in the drastic reduction of methane yield. Table 4 shows the elemental analysis of the digestate after the AD process of the **FRC** test. Several limits have been reported in the literature for observed inhibition and toxicity of some heavy metals. Although some variations may be found, due mostly to inoculum acclimation, chemical forms and substrate source, a rough extrapolation could be accepted. For example, Alrawashdeh et al. (2020) reported toxic limits for Fe, Ni, Pb, Zn, Cu and Cr of >1.45 mg dm^{-3}, >0.041 mg dm^{-3}, >1.27 mg dm^{-3}, ≥0.29 mg dm^{-3}, ≥562.5 mg dm^{-3} and ≥0.692 mg dm^{-3}, respectively. Silva et al. (2021) additionally reported AD inhibition due to Se concentrations of 0.059–1.639 mg dm^{-3}, although they reported beneficial effects when the digestate was supplemented with Fe at final concentrations in the digestate as high as 120 mg dm^{-3}. Abdel-Shafy and Mansour (2014) observed initial inhibitions of the AD at concentrations of Hg, Cd and Cr as low as 0.025 ppm d.m., 0.155 ppm d.m. and 0.034 ppm d.m., respectively. Paulo et al. (2017) reported that Ni and Co had a negative effect on the methanogenic microorganisms at concentration of 8 mM and 30 mM, respectively. Chen et al. (2007) reported that generally the relative sensitivity of the acidogenesis step to heavy metals is Cu > Zn > Cr > Cd > Ni > Pb, while for methanogenesis the order slightly changed to Cd > Cu > Cr > Zn > Pb > Ni. Nevertheless, as can be seen in Table 4, the digestate showed concentrations of the previously mentioned elements higher than those reported as toxic, with the exception of Se, which was not determined, and Cu, which was within the range of being innocuous for the AD process as described by Silva et al. (2021).

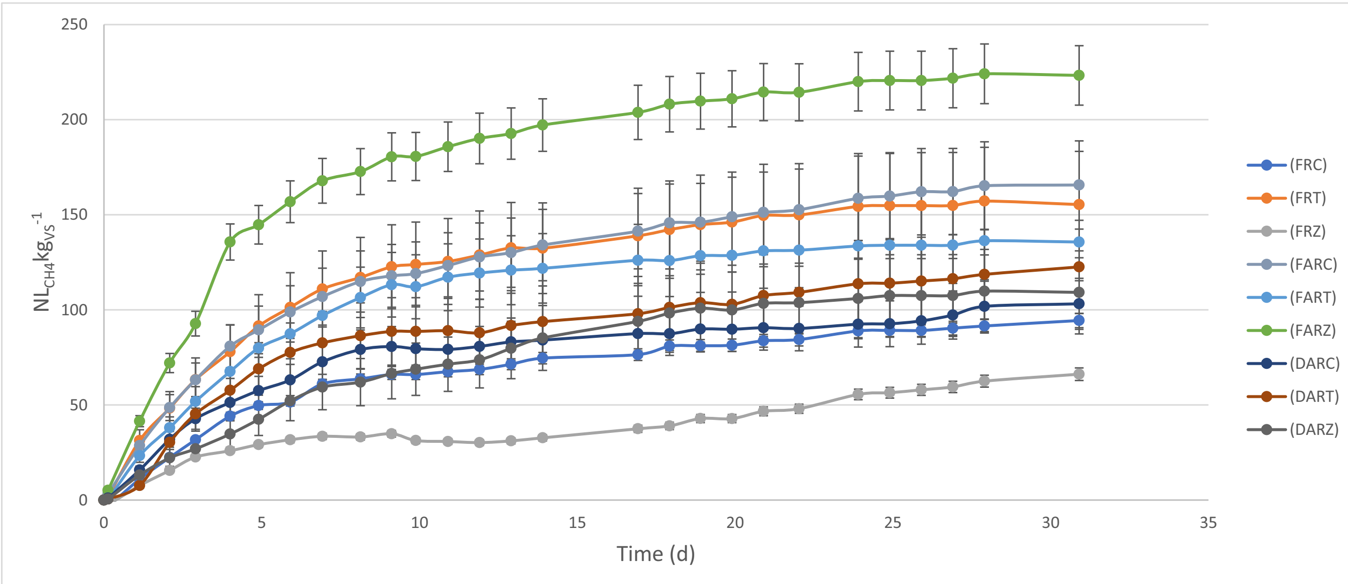

Fig. 2. Methane yield versus time of different tests assayed.
FRC: Untreated Fresh *Rugulopteryx okamurae* (*R.o.*) as Control; **FRT**: Fresh *R.o.* Thermally pretreated; **FRZ**: Fresh *R.o.* milled with zeolite; **FARC**: Untreated Fresh Ashore *R.o.* as Control; **FART**: Fresh Ashore *R.o.* Thermally pretreated; **FARZ**: Fresh Ashore *R.o.* milled with zeolite; **DARC**: Untreated Dried Ashore *R.o.* as Control; **DART**: Dried Ashore *R.o.* Thermally pretreated; **DARZ**: Dried Ashore *R.o.* milled with zeolite.

Table 4
Elemental and metal compositions of FRC digestate after the AD process.

Parameter[a]	Liquid phase	Solid phase	Total digestate	Europe[1]	UK[2]	USA[3]
B (ppm)	36 (5)	160 (10)	39 (8)	–	–	–
Na (g kg^{-1})	1.44 (0.08)	10 (1)	1.7 (0.7)	–	–	–
Mg (g kg^{-1})	0.20 (0.02)	4.9 (0.2)	0.3 (0.1)	–	–	–
Al (g kg^{-1})	0.07 (0.02)	1.9 (0.2)	0.1 (0.1)	–	–	–
P (g kg^{-1})	<LOQ[b]	<LOQ	<LOQ	–	–	–
K (g kg^{-1})	3.0 (0.1)	13 (1)	3.3 (0.7)			
Ca (g kg^{-1})	8 (1)	45 (6)	9 (4)	–	–	–
Cr (ppm)	5 (2)	60 (10)	6 (7)	70	8–80	–
Mn (ppm)	4.0 (0.7)	50 (10)	5 (7)	–	–	–
Fe (g kg^{-1})	0.058 (0.005)	4.8 (0.4)	0.2 (0.3)	–	–	–
Co (ppm)	0.22 (0.06)	24 (4)	1 (3)	–	–	–
Ni (ppm)	4 (1)	70 (10)	6 (7)	25	4–40	420
Cu (ppm)	<LOQ	53 (4)	1 (4)	70	16–160	1500
Zn (ppm)	21 (3)	530 (60)	30 (40)	200	32–320	2800
As (ppm)	0.50 (0.02)	3.9 (0.7)	0.6 (0.5)	–	–	41
Mo (ppb)	<LOQ	25,000 (1000)	700 (1000)	–	–	–
Cd (ppb)	160 (70)	5900 (300)	300 (200)	700	120–1200	39,000
Sn (ppb)	570 (70)	6500 (400)	700 (300)	–	–	–
Ba (ppm)	98 (4)	210 (60)	100 (40)	–	–	–
Hg (ppm)	19 (4)	30 (6)	19 (5)	0.4	0.08–0.8	17
Pb (ppm)	7 (2)	210 (20)	12 (14)	45	16–160	300

[a] Value represent mean (standard error). Results based on dry matter.
[b] Limit of quantification.
[1] Saveyn and Eder, 2014.
[2] United Kingdom – BSI PAS 110:2014. Values range depends on Total Nitrogen content of the biomass.
[3] US EPA Regulation CFR40/503.

Another plausible interpretation could be linking methane production with the C/N ratio. It has been widely studied the effect of this ratio on AD performance, being the accepted optimum value between 25 and 30 (Paul and Dutta, 2018). It is generally accepted that C/N $<$ 20, at a pH higher than 7.4, increases the production of free ammonia nitrogen which is a powerful inhibitor of the AD process (Yenigün and Demirel, 2013). However, as described above, all the reactors showed a total ammonium nitrogen significantly below the established limit for inhibition. Nevertheless, a better-balanced C/N ratio could enhance methane production, which is confirmed by the higher yield obtained from the FARZ test, with the second highest ratio (19.2). However, the FART sample with an even higher ratio (22.6) showed a lower yield and a similar heavy metal profile. This could be explained by the zeolite effect which reduced the crystallinity of the cellulose fraction, allowing for better access to the hydrolytic enzymes during the AD process (De la Lama-Calvente et al., 2023).

3.3. Estimation of the model parameters by kinetic modelling

3.3.1. First-order kinetic model

Table 5 reports the parameters determined by the eq. S1 for the different experiments. The small values of the standard deviations,

Table 5
Values of the kinetic constant obtained from the first-order model for the different R.o. biomasses tested. Figures within brackets represent the standard deviations.

Substrate	G_{max} (NL_{CH4} kg_{VS}^{-1})	k ($days^{-1}$)	R^2	S.E.E.	Error (%)
FRC	90 (1)	0.14 (0.00)	0.994	3.154	4.6 %
FRT	153 (1)	0.18 (0.00)	0.997	3.516	2.4 %
FRZ	64 (6)	0.07 (0.01)	0.958	6.549	3.2 %
FARC	160 (2)	0.15 (0.00)	0.995	5.100	3.3 %
FART	135 (1)	0.18 (0.00)	0.998	2.071	0.4 %
FARZ	217 (2)	0.20 (0.00)	0.996	5.932	2.8 %
DARC	93 (1)	0.19 (0.00)	0.993	3.480	8.6 %
DART	113 (2)	0.16 (0.00)	0.988	5.609	7.3 %
DARZ	119 (1)	0.09 (0.00)	0.998	2.041	8.9 %

FRC: Untreated Fresh *R.o.* as Control; **FRT**: Fresh *R.o.* Thermally pretreated; **FRZ**: Fresh *R.o.* milled with zeolite; **FARC**: Untreated Fresh Ashore *R.o.* as Control; **FART**: Fresh Ashore *R.o.* Thermally pretreated; **FARZ**: Fresh Ashore *R.o.* milled with zeolite; **DARC**: Untreated Dried Ashore *R.o.* as Control; **DART**: Dried Ashore *R.o.* Thermally pretreated; **DARZ**: Dried Ashore *R.o.* milled with zeolite. *R.o.*: *Rugulopteryx okamurae*; S.E.E.: Standard Error of Estimate; G_{max}: Ultimate methane production (NL_{CH4} kg_{VS}^{-1}); k: specific rate constant or apparent kinetic constant ($days^{-1}$); R^2: Determination coefficient; Error (%): difference (in percentage) between the experimental and calculated ultimate methane production.

standard errors of estimates and the percentages of errors, and the high determination coefficient values (>0.991) prove the adequate fit of the experimental results to the theoretical model. In order to facilitate the discussion, the three different initial samples have been considered separately.

3.3.1.1. Natural fresh R.o. (FR) biomass. The k and G_m values increased by 28.5 % and 70 % higher, respectively, when the biomass was subjected to the thermal treatment. By contrast, both kinetic parameters decreased considerably by using zeolite during the milling process. For instance, G_m value of **FRZ** diminished 28.8 % and 58.1 % when compared to the values achieved for **FRC** and **FRT**, respectively. The low k values observed for **FRZ** may be attributed to the release of inhibitory substances after treatment with zeolite such as recalcitrant organic compounds or the heavy metals present in the algae. Additionally, the competition for electron donors between sulphate-reducing bacteria and acetoclastic methanogens may have a significant influence as well (Cogan and Antizar-Ladislao, 2016), although further investigation would be required in order to confirm this phenomenon which was outside the scope of this study.

Lower kinetic constant values were reported in BMP experiments of *Pelvetia canaliculate* (0.11 $days^{-1}$), a brown macroalgae collected in the Isle of Bute, Scotland (Rodriguez et al., 2018). On the contrary, higher k values (0.31 $days^{-1}$) were reported by Membere and Sallis (2018) in BMP experiments carried out with *Laminaria digitata* at 35 °C. The higher k values achieved for *L. digitata* AD mean a shorter degradation time and this fact could be a result of the rapid acclimatization of the inoculum at this temperature (Membere and Sallis, 2018).

3.3.1.2. Fresh ashore R.o. (FAR) biomass. **FART** and **FARZ** tests increased the kinetic constant (k) value by 20.2 % and 33.3 %, respectively, compared with the untreated sample (**FARC**). In addition, the kinetic constant values achieved for **FARC** and **FART** were virtually identical to those achieved for their equivalent **FRC** and **FRT**. Similar k values to those achieved in the present work were found in a thermophilic BMP test of *Sargassum fulvellum* used either untreated (0.18 ± 0.03 $days^{-1}$) or pretreated enzymatically (0.16 ± 0.03 $days^{-1}$) (Farghali et al., 2021).

However, the extraction of sap, ulvan and protein prior the BMP test increased the kinetic constant of the green seaweed *Ulva lactuca* from 0.15 $days^{-1}$ to 0.28 $days^{-1}$ (Mhatre et al., 2019). This study corroborates that high protein and sulphate content are major inhibitors in the AD of *Ulva lactuca* which could be the reason of the low value observed for **FRC** and **FARC** (Mhatre et al., 2019).

In relation to the G_m value, the **FARZ** sample also achieved the highest value (217 (2) NL_{CH4} kg_{VS}^{-1}), which was 35.6 % and 60.7 % higher than those obtained for **FARC** and **FART**, respectively. This is in contrast with the results observed for **FR** (fresh *R.o.*), where the addition of zeolite during the milling step significantly reduces the kinetics parameters. However, as shown in Table 2, **FAR** presented lower content of most of the analysed elements (e.g. Al, K, Ca, Cr, Cu, As, Cd, Sn, Pb), suggesting that the observed difference may be attributed to the inhibition produced by these elements.

3.3.1.3. Dried ashore R.o. (DAR) biomass. The kinetic constants of the dried samples showed a different trend compared to those observed previously. Specifically, the k value of the **DARZ** sample decreased 52.6 % and 43.7 % with respect to the values achieved for **DARC** and **DART**, respectively. Moreover, the k values for **DART** and **DARZ** were lower than the equivalent values obtained for the fresh ashore biomasses **FART** and **FARZ**. The same trend was observed for the G_m values when comparing both groups of ashore *R.o.* biomasses (Fresh and Dried).

As was previously stated in the cases of the **FR** biomasses, the low k values observed for **DARZ** compared with the other two substrates may be attributed to the presence of inhibitory substances after treatment with zeolite such as persistent organic contaminants as well as to the low values of the C/N ratio (10.7–12.1) compared to more appropriate values in the fresh ashore biomasses (19.2–22.6) (Cogan and Antizar-Ladislao, 2016). Moreover, **DAR** samples showed a similar elemental profile to **FR**, in contrast with **FAR**, which showed a lower content for most of the elements determined. This supports the idea of zeolite increasing the surface contact of the biomass to the anaerobic microbiota and thus releasing the toxic heavy metals.

3.3.2. Transference function model

Table 6 shows the transference function model parameters obtained in this study. The parameters were assessed using the nonlinear regression approach. As with the first-order model, the experimental data adequately fit the proposed model. The high accuracy of prediction

Table 6
Values of the parameters obtained from the Transference Function model for the different *R.o.* biomasses studied. Figures within brackets represent the standard deviations.

Substrate	B_m (NL_{CH4} kg_{VS}^{-1})	R_m (NL_{CH4} kg_{VS}^{-1} d^{-1})	ʎ (d)	R^2	S.E.E.	Error (%)
FRC	90 (1)	12.7 (0.5)	4.0 • 10^{-10}	0.994	3.217	4.5 %
FRT	153 (1)	26.6 (0.8)	6.9 • 10^{-10}	0.997	3.769	2.7 %
FRZ	64 (7)	4.7 (0.6)	1.6 • 10^{-8}	0.948	6.679	3.2 %
FARC	160 (2)	24 (1)	1.9 • 10^{-9}	0.995	5.201	3.3 %
FART	134.4 (0.7)	24.6 (0.4)	0.096	0.999	1.964	0.9 %
FARZ	217 (2)	44 (2)	1.7 • 10^{-10}	0.996	6.096	2.7 %
DARC	94 (1)	18.0 (0.9)	0.005	0.993	3.549	8.7 %
DART	113 (2)	19 (1)	0.068	0.988	5.933	7.3 %
DARZ	120 (2)	10.7 (0.2)	3.2 • 10^{-10}	0.998	2.048	9.0 %

FRC: Untreated Fresh *R.o.* as Control; **FRT**: Fresh *R.o.* Thermally pretreated; **FRZ**: Fresh *R.o.* milled with zeolite; **FARC**: Untreated Fresh Ashore *R.o.* as Control; **FART**: Fresh Ashore *R.o.* Thermally pretreated; **FARZ**: Fresh Ashore *R.o.* milled with zeolite; **DARC**: Untreated Dried Ashore *R.o.* as Control; **DART**: Dried Ashore *R.o.* Thermally pretreated; **DARZ**: Dried Ashore *R.o.* milled with zeolite. *R.o.*: *Rugulopteryx okamurae*; B_m: is the ultimate methane production; R_m: is the maximum methane production rate; ʎ is the lag time. S.E.E.: Standard Error of Estimate; R^2: Determination coefficient; Error (%): difference (in percentage) between the experimental and calculated ultimate methane production.

for the methane production by the model implies that future analysis will suit within the predicted outcome for the tested samples. The observed lag times (ʎ), close to zero across the board, indicate a fast degradation of the most available components. As before, in order to facilitate the discussion, the three different initial samples have been considered separately.

3.3.2.1. Natural fresh R.o. (FR) biomass. **FRT** reached a maximum methane production rate (R_m) value 109.4 % higher than that found for the untreated biomass (**FRC**). In addition, the B_m value was also 70 % higher when the biomass was thermally pretreated compared with the untreated test. This result could be explained by the fact that the application of a thermal pretreatment to the macroalgae prior to AD facilitates the disintegration of the biomass macrostructure (Barbot et al., 2015). By contrast, the lowest values for both parameters were found for the **FRZ**, which may be attributed to the same reasons expressed in the first-order model section. Additionally, the Hg concentration contained in **FR** was 31.0 (0.4) ppm, a value higher than those present in **FAR** or **DAR**.

3.3.2.2. Fresh ashore R.o. (FAR) biomass. The performance and kinetic behaviour observed for both **FARC** and **FART** were identical (24 (1) and 24.6 (0.4) NL_{CH4} kg_{VS}^{-1} d^{-1}, respectively) and very similar to the value found in the AD of the macroalga *Ulva lactuca* using cow manure as inoculum (R_m value of 24.4 NL_{CH4} kg_{VS}^{-1} d^{-1}) which slightly increased after the pretreatment with ozone at doses of 249 g ozone kg_{VS}^{-1} of algal biomass (Hassaan et al., 2021). However, after the zeolite-assisted milling process an increase of 80.5 % in the R_m value (43.7 NL_{CH4} kg_{VS}^{-1} d^{-1}) was observed in the present study. This fact may be attributed to the appropriate C/N ratio of **FARZ**, which was very close to 20, while the values of this ratio for the other two biomasses were lower (around 17).

Similar R_m values (48 ± 1 NL_{CH4} $kg_{VS}^{-1}d^{-1}$) to that for **FARZ** were reported by Ap et al. (2021) when the *Sargassum fulvellum* biomass was used as feedstock for the batch AD process and it was mechanically pretreated to reduce the particle size from 106 μm–4.75 mm to 75–850 μm. In addition, in this case, and similar to that occurred in the present research the rate of hydrolysis and maximum biomethane production potential improved after mechanical pretreatment by a maximum of 45.60 % and 48.71 %, respectively (Ap et al., 2021).

3.3.2.3. Dried ashore R.o. (DAR) biomass. Both the values of B_m and R_m for **DARC**, **DART**, and **DARZ** were lower than those obtained for the three fresh ashore biomasses. The lowest value of R_m (10.7 (0.2) NL_{CH4} kg_{VS}^{-1} d^{-1}) was found for **DARZ**, which was 40.5 % lower than that obtained for **DARC**. This lower value of the kinetic parameter R_m found for the **DARZ** compared to the value observed for the **FARZ** may be attributed to the lower value of the C/N ratio (12.1 and 19.2, respectively) as well as the differences in the elemental profile, where **FAR** samples showed lower content of most of the toxic heavy metals discussed above (e.g. Sn, Cd, Pb, Hg).

The highest R_m value (19 (1) NL_{CH4} kg_{VS}^{-1} d^{-1}) was found for **DART**. Higher R_m values (72.4 L_{CH4} kg_{VS}^{-1} d^{-1}) were reported by Lin et al. (2019) in BMP experiments of the dried seaweed *Saccharina latissima* after a hydrothermal pretreatment at a temperature of 140 °C for 30 min and a dark fermentation during 48 h for hydrogen production. In this case, FTIR spectra of *S. latissima* biomass before and after hydrothermal pretreatment revealed that the complex structural components of *S. latissima* can be partially transformed from water-insoluble fraction (macromolecular polymers) to water-soluble fraction (low molecular weight organics such as mannitol and glucose), thereby increasing the soluble COD production during hydrothermal pretreatment. However, this study also demonstrated that an increase in the temperature of the thermal pretreatment to 180 °C brought about a decrease in the R_m value to 52.6 L_{CH4} kg_{VS}^{-1} d^{-1} which may be attributed to the transformation of sugars and aminoacids contained in the algal biomass which could also cause binary interactions between the carbonyl group (C═O) and amino group (—NH_2), leading to the generation of various fermentative inhibitors (such as methyl furfural, pyrazine compounds, and nitrogen-containing Maillard compounds) (Lin et al., 2019).

3.3.3. Overall considerations about the kinetic parameters

The biomass conversion into methane has been assessed by the kinetic parameters obtained from the experimental data through the two models assayed, which aid in the further design and optimization of the higher-scale anaerobic process (Rose-Benish et al., 2022). These parameters help determining the needed time of the anaerobic microorganisms to acclimate to the substrate, as well as to provide an insight of the length of the digestion period and the ability of the substrate to biodegrade. Therefore, these kinetic parameters serve as indicators for evaluating the performance of the anaerobic reactor (Fernández-Rodríguez et al., 2022). The kinetic constants, k (first-order model) and R_m (TF model), offers an insight on how quickly the biomethanization process would be carried out, thus, higher values, would represent potentially lower hydraulic retention times with higher organic retention times in scaled-up systems as the substrate is degraded with less difficulty. Moreover, the lag time observed from the TF model could be linked to the acclimatization of the inoculum to the substrate and the length of the limiting-step hydrolysis which would be translated in longer start-up periods in industrial systems. Nevertheless, these models would need to be coupled with mass balances equations which are specific and dependent on the plant configuration in real cases (Ekama et al., 2007). In any case, a kinetic study is a useful tool for comparison assuming the reactor design is the same for all the cases. For instance, in this study, the best values were obtained for the FARZ sample, which is in accordance with the other parameters investigated, such as the BMP or the biodegradability, suggesting that this sample would be the best candidate for further investigations in scale-up systems.

3.4. Anaerobic digestate and its potential use as a biofertilizer

Several studies have revealed the presence of heavy metals in different species of macroalgae. In fact, many of these species have been used as bioindicators of the presence of these pollutants in water, being highly dependent on the specie and geographical location (Jeong and Ra, 2022).

The use of macroalgae directly as fertilizer has been assessed in previous studies, with the presence of heavy metals being one of the main drawbacks (Rakib et al., 2021). The maximum allowable content of heavy metals in fertilizers depends on each country. Table 4 shows the maximum allowable concentration in fertilizer, for each heavy metal, in Europe, UK and USA.

Table 3 shows the heavy metals content of the three substrates used in this experiment. The Cr, Ni, Cu and Hg contents are above the limits established in the current legislations on the use of fertilizers. The heavy metals concentration is even higher in dry ashore biomass, where the drying natural process has acted as a toxic element's concentrator. It is worth mentioning the high Hg substrates content (of 3 biomasses studied), whose concentration was higher than 20 ppm in all cases, reaching a concentration of 31.0 (0.4) ppm in natural *R.o.* biomass. European fertilizer legislation does not allow concentrations >0.4 ppm of Hg (Table 4). Values between 0.30 and 4.68 ppm of Hg were reported by Ferreira (1991) in different macroalgae species collected at the Tagus estuary (Portugal). Macroalgae Hg concentration depends on both, temporal and spatial variables (Ferreira, 1991). Regardless of the degree of contamination of the study area, the rhodophytes Hg concentration was always higher than in the other groups of macroalgae due to physiological and biological characteristics (Ferreira, 1991).

The As and Cd content of biomass, was only higher than the limits established in the current legislation in the **DAR** biomass (54 (7) and 940 (70) ppm, respectively). While the Cd and As content of the **FR** biomass was 660 (6) and 27 (4), respectively and 130 (10) and 17 (2) for the **FAR** biomass Cd and As content, respectively. Jeong and Ra (2022) reported much lower values for Cr, Ni, Cu, Zn, As, Cd and Pb in the green macroalga *Halimeda* from Chuuk, Micronesia. Boundir et al. (2022) also reported both seasonal and spatial variability in heavy metals macroalgae concentrations. Boundir et al. (2022) used *Ericaria selaginoides* (pheophyceae) as biomonitoring for heavy metal concentration of the Moroccan coast. Values of up to Cd concentration of 1.18 $\pm$ 0.09 ppb; Pb of 3.26 $\pm$ 0.83 ppb, Cu of 0.75 $\pm$ 0.13 ppb and Cr of 1.12 $\pm$ 0.15 ppb were reported in two polluted stations of the study area (Boundir et al., 2022).

Anaerobic digestion is a key process for the reuse of organic by-products and, therefore, for the circular economy (Magnusson et al., 2022). After the AD process, the generated stabilized digestate could be used as fertilizer, although, the need to reuse this digestate is one of the main bottlenecks of the large-scale anaerobic process (Magnusson et al., 2022). This is because the digestate properties depend mainly on the feedstock used in the process (Monlau et al., 2015) and in the case of algae feedstock, the presence of heavy metals which may be outside the permitted limits (Stürmer et al., 2020).

Table 4 shows the elemental analysis of the two different phases of the digestate (i.e. solid and liquid fraction) as well as the total content. Although the macroalgae raw material had high heavy metals concentrations such as Hg, Cu, Ni, Cr, As and Cd; only Hg values above those established in current European legislation were found in the total digestate (Table 4). A similar trend was found in the liquid part of the digestate, where the Hg values obtained (19 (4) ppm) were well above those allowed by the fertilizer European law (0.4 ppm). On the other hand, in the solid part, values above the permitted levels were found for Zn, Cd, Hg and Pb (Table 4). Previous studies have already reported a decrease in macroalgae anaerobic digestate heavy metal content (Nkemka and Murto, 2010).

In addition, the use of pre-treatments to retain heavy metals of macroalgae digestate has also been studied in order to use this type of digestate as fertilizer (Nkemka and Murto, 2010). The most widely used methods for heavy metals removal in wastewater are bioadsorbents, although others are currently being studied, such as carbon-based methods or silicate binders, which are proving to be very efficient, safe and low-cost methods for heavy metals removal (Rakib et al., 2021).

4. Conclusions

In this study, the impact of the life cycle and natural degradation of the invasive alien brown macroalgae *Rugulopteryx okamurae* on the anaerobic digestion (AD) have been assessed through BMP tests for the first time. Differences observed in the physicochemical characterization (moisture, VS, C/N ratio, etc.) of the different substrates were related to their natural location, life cycle of the specie and/or natural composting by local micro and macro biota.

All the studied samples presented heavy metal levels above the inhibition/toxic limits for AD. Low methane yield and biodegradability have been reported for almost all the assays investigated. Moreover, the generated digestates are not suitable for directly being used as a biofertilizer.

Data from AD experiments of the *R.o.* biomasses were well described by the kinetic models. An increase in the first-order kinetic constant (k) values were observed for the **FRC** and **FARC** biomasses when these were subjected to thermal pretreatment. By contrast, for the dried biomass a decrease in the k value was detected. The highest value of the maximum methane production rate (R_m) (TF model) was achieved for the **FARZ** sample, which was due potentially to its adequate C/N ratio, very close to the optimum ratio for AD processes and its lower content of toxic heavy metals. Thermal pretreatments although enhanced the methane yield in some cases (**FRT** and **DART**) are not economically viable. However, zeolite-assisted milling treatment greatly enhanced the methane yield of the fresh ashore biomass and the economic profit of the AD.

Finally, this study shows that even in a scenario where macroalgae are highly contaminated by heavy metals, the best AD performance would be carried out by collecting the algae when freshly arrived on the shore. Besides, the use of zeolite as an abrasive during the milling process enhances methane production and the profits of the overall process. Moreover, an additional benefit, not included in the economic assessment, would be the abatement of the negative impacts of *R.o.* biomass in a number of coastal areas located in the south of Spain, making the overall process more sustainable and profitable.

CRediT authorship contribution statement

David De la Lama-Calvente: Conceptualization, Data curation, Investigation, Methodology, Supervision, Visualization, Writing – original draft. **María José Fernández-Rodríguez:** Conceptualization, Data curation, Investigation, Methodology, Supervision, Validation, Writing – original draft. **José Carlos García-Gómez:** Conceptualization, Data curation, Formal analysis, Investigation, Supervision, Validation, Writing – original draft. **Rafael Borja:** Conceptualization, Data curation, Funding acquisition, Investigation, Methodology, Resources, Supervision, Validation, Writing – original draft.

Declaration of competing interest

The authors declare that they have no known competing financial interests or personal relationships that could have appeared to influence the work reported in this paper.

Data availability

Data will be made available on request.

Acknowledgements

The authors wish to express their gratitude to Lisa Souvre for her fundamental assistance on the experimental procedure. We also wish to thank Dr. Menta Ballesteros and Dr. Ángel Rabdel Ruiz-Salvador for providing zeolite samples and scientific and technical support. Finally, the authors wish to express their gratitude to the Spanish Ministry of Science and Innovation for providing financial support through the project PID2020-114975RB-100/AEI/10.13039/5011000/11033. M.J. F-R is recipient of a “Juan de la Cierva Formación” grant from the Spanish State Research Agency (FJC2020-045654-I).

Appendix A. Supplementary data

Supplementary data to this article can be found online at https://doi.org/10.1016/j.marpolbul.2023.115005.

References

Abdel-Shafy, H.I., Mansour, M.S.M., 2014. Biogas production as affected by heavy metals in the anaerobic digestion sludge. Egypt. J. Pet. 23, 409–417. https://doi.org/10.1016/j.ejpe.2014.09.009.

Adams, J.M.M., Toop, T.A., Donnison, I.S., Gallagher, J.A., 2011. Seasonal variation in Laminaria digitata and its impact on biochemical conversion routes to biofuels. Bioresour. Technol. 102 (21), 9976–9984. https://doi.org/10.1016/j.biortech.2011.08.032.

Alrawashdeh, K.A., Gul, E., Yang, Q., Yang, H., Bartocci, P., Fantozzi, F., 2020. Effect of heavy metals in the performance of anaerobic digestion of olive mill waste. Processes 8 (9), 1146. https://doi.org/10.3390/pr8091146.

Alvarado-Morales, M., Gunnarsson, I.B., Fotidis, I.A., Vasilakou, E., Lyberatos, G., Angelidaki, I., 2015. Laminaria digitata as a potential carbon source for succinic acid and bioenergy production in a biorefinery perspective. Algal Res. 9, 126–132. https://doi.org/10.1016/j.algal.2015.03.008.

Anderson, L.W., 2005. California's reaction to Caulerpa taxifolia: a model for invasive species rapid response. Biol. Invasions 7 (6), 1003–1016. https://doi.org/10.1007/s10530-004-3123-z.

Ap, Y., Farghali, M., Mohamed, I.M.A., Iwasaki, M., Tangtaweewipat, S., Ihara, I., Sakai, R., Umetsu, K., 2021. Potential of biogas production from the anaerobic digestion of Sargassum fulvellum macroalgae: influences of mechanical, chemical, and biological pretreatments. Biochem. Eng. J. 175, 108140 https://doi.org/10.1016/j.bej.2021.108140.

APHA, 2017. Standard methods for the examination of water and wastewater, 23rd ed. American Public Health Association, American Water Works Association, Water Environment Federation, Washington DC.

Ayala-Mercado, I.D., Weber, B., Durán-García, M.D., 2021. Use of hydrothermal pretreatment to enhance biogas production from pelagic sargassum. BioEnergy Res. 15, 1639–1648. https://doi.org/10.1007/s12155-021-10371-4.

Barbot, I.N., Thomsen, L., Benz, R., 2015. Thermo-acidic pretreatment of beach macroalgae from Rügen to optimize biomethane production—Double benefit with simultaneous bioenergy production and improvement of local beach and waste management. Mar. Drugs 13, 5681–5705. https://doi.org/10.3390/md13095681.

Bogolitsyn, K., Parshina, A., Aleshina, L., 2020. Structural features of brown algae cellulose. Cellulose 27, 9787–9800. https://doi.org/10.1007/s10570-020-03485-z.

Boundir, Y., Haroun, R., Sánchez-de Pedro, R., Hasni, M., Ouazzani, N., Mandi, L., Rafig, F., Weinberger, F., Cherifi, O., 2022. Biomonitoring of heavy metal pollution using the brown seaweed Ericaria selaginoides along the Atlantic coast of Morocco. Appl. Ecol. Environ. Res. 20 (1), 21–41. https://doi.org/10.15666/aeer/2001_021041.

Brown, A.E., Finnerty, G.L., Camargo-Valero, M.A., Ross, A.B., 2020. Valorisation of macroalgae via the integration of hydrothermal carbonisation and anaerobic digestion. Bioresour. Technol. 312, 123539 https://doi.org/10.1016/j.biortech.2020.123539.

Casal-Porras, I., Zubía, E., Brun, F.G., 2021. Dilkamural: a novel chemical weapon involved in the invasive capacity of the alga rugulopteryx okamurae in the strait of Gibraltar. Estuar. Coast. Shelf Sci. 257, 107398 https://doi.org/10.1016/j.ecss.2021.107398.

Casallas-Ojeda, M., Meneses-Bejarano, S., Urueña-Argote, R., Marmolejo-Rebellón, L.F., Torres-Lozada, P., 2022. Techniques for quantifying methane production potential in the anaerobic digestion process. Waste Biomass Valor. 13, 2493–2510. https://doi.org/10.1007/s12649-021-01636-2.

Chen, Y., Cheng, J.J., Creamer, K.S., 2007. Inhibition of anaerobic digestion process: a review. Bioresour. Technol. 99, 4044–4064. https://doi.org/10.1016/j.biortech.2007.01.057.

Choi, S., Kim, S.I., Yulisa, A., Aghasa, A., Hwang, S., 2023. Proactive prediction of total volatile fatty acids concentration in multiple full-scale food waste anaerobic digestion systems using substrate characteristics with machine learning and feature analysis. Waste Biomass Valor. 14, 593–608. https://doi.org/10.1007/s12649-022-01826-6.

Chynoweth, D.P., 1981. Microbial conversion of biomass to methane. In: Energy Technology: Proceedings of the Energy Technology Conference, pp. 1281–1305. ISBN: 086587008X.

Cogan, M., Antizar-Ladislao, B., 2016. The ability of macroalgae to stabilise and optimise the anaerobic digestion of household food waste. Biomass Bioenergy 86, 146–155. https://doi.org/10.1016/j.biombioe.2016.01.021.

Darko, C.N.S., Agyei-Tuffour, B., Faloye, D.F., Goosen, N.J., Nyankson, E., Dodoo-Arhin, D., 2022. Biomethane production from residual algae biomass (Ecklonia maxima): effects of inoculum acclimatization on yield. Waste Biomass Valoriz. 13, 497–509. https://doi.org/10.1007/s12649-021-01497-9.

De la Lama-Calvente, D., Fernández-Rodríguez, M.J., Ballesteros, M., Ruiz-Salvador, Á. R., Raposo, F., García-Gómez, J.C., Borja, R., 2023. Turning an invasive alien species into a valuable biomass: anaerobic digestion of rugulopteryx okamurae after thermal and new developed low-cost mechanical pretreatments. Sci. Total Environ. 856, 158914 https://doi.org/10.1016/j.scitotenv.2022.158914.

Ding, L., Cheng, J., Lin, R., Deng, C., Zhou, J., Murphy, J.D., 2020. Improving biohydrogen and biomethane co-production via two-stage dark fermentation and anaerobic digestion of the pretreated seaweed Laminaria digitata. J. Clean. Prod. 251, 119666 https://doi.org/10.1016/j.jclepro.2019.119666.

EC, 2022. EU Eurostat – Statistics Explained. https://ec.europa.eu/eurostat/statistics-explained/index.php?title=Electricity_price_statistics. (Accessed 9 September 2022).

EIA, 2022. Electricity data browser - average retail price of electricity. In: U.S. Energy Information Administration. eia.gov. (Accessed 9 September 2022).

Ekama, G.A., Sotemann, S.W., Wentzel, M.C., 2007. Biodegradability of activated sludge organics under anaerobic conditions. Water Res. 41, 244–252. https://doi.org/10.1016/j.watres.2006.08.014.

El Aamri, F., Idhalla, M., Tamsouri, M.N., 2018. Occurrence of the invasive brown seaweed Rugulopteryx okamurae (E.Y.Dawson) I.K.Hwang, W.J. Lee & H.S.Kim (Dictyotales, Phaeophyta) in Morocco (Mediterranean Sea). In: MedFAR, 1 (2), pp. 92–96.

El Nemr, A., Hassaan, M.A., Elkatory, M.R., Ragab, S., Pantaleo, A., 2021. Efficiency of Fe3O4 nanoparticles with different pretreatments for enhancing biogas yield of macroalgae Ulva intestinalis linnaeus. Molecules 25, 5105. https://doi.org/10.3390/molecules26165105.

Fabre, E., Dias, M., Henriques, B., Viana, T., Ferreira, N., Soares, J., Pinto, J., Vale, C., Pinheiro-Torres, J., Silva, C.M., Pereira, E., 2021. Bioaccumulation processes for mercury removal from saline waters by green, brown and red living marine macroalgae. Environ. Sci. Pollut. Res. 28, 30255–30266. https://doi.org/10.1007/s11356-021-12687-2.

Farghali, M., AP, Y., Mohamed, I.M.A., Iwasaki, M., Tangtaweewipat, S., Ihara, I., Sakai, R., Umetsu, K., 2021. Thermophilic anaerobic digestion of Sargassum fulvellum macroalgae: Biomass valorization and biogas optimization under different pre-treatment conditions. J. Environ. Chem. Eng. 9, 106405 https://doi.org/10.1016/j.jece.2021.106405.

Faria, J., Prestes, A.C.L., Moreu, I., Cacabelos, E., Martins, G.M., 2022. Dramatic changes in the shallow-water marine benthic communities following the invasion by rugulopteryx okamurae (Dictyotales, Ochraphyta) in Azores (NE Atlantic). Mar. Pollut. Bull. 175, 113358 https://doi.org/10.1016/j.marpolbul.2022.113358.

Fernández-Rodríguez, M.J., Cubero-Cardoso, J., de la Lama-Calvente, D., Fernández-Prior, A., Rodríguez-Gutiérrez, G., Borja, R., 2022. Anaerobic digestion of the residue (combination of wastewater and solid waste) from a new olive-oil manufacturing process based on an olive cold-pressing system: kinetic approach and process performance. Processes 10 (12), 2552. https://doi.org/10.3390/pr10122552.

Fernández-Rodríguez, M.J., de la Lama-Calvente, D., Jiménez-Rodríguez, A., Pino-Mejías, R., Borja, R., Rincón, B., 2020. Impact of soft hydrothermal pre-treatments on the olive mill solid waste characteristics and its subsequent anaerobic digestion. Biomass Conv. Bioref. https://doi.org/10.1007/s13399-020-00759-1.

Ferreira, J.G., 1991. Factors governing mercury accumulation in three species of marine macroalgae. Aquat. Bot. 39 (3–4), 335–343. https://doi.org/10.1016/0304-3770(91)90007-R.

Gao, S., Zhang, R., Zhang, H., Zhang, S., 2022. The seasonal variation in heavy metal accumulation in the food web in the coastal waters of Jiangsu based on carbon and nitrogen isotope technology. Envrion. Pollut. 297, 118649 https://doi.org/10.1016/j.envpol.2021.118649.

García-Gómez, J.C., Florido, M., Olaya-Ponzone, L., Sempere-Valverde, J., Megina, C., 2021. The invasive macroalga rugulopteryx okamurae: substrata plasticity and spatial colonization pressure on resident macroalgae. Front. Ecol. Evol. 9, 631754 https://doi.org/10.3389/fevo.2021.631754.

García-Gómez, J.C., Sempere-Valverde, J., González, A.R., Martínez-Chacón, M., Olaya-Ponzone, L., Sánchez-Moyano, E., Ostalé-Valriberas, E., Megina, C., 2020. From exotic to invasive in record time: the extreme impact of rugulopteryx okamurae (Dictyotales, Ochrophyta) in the strait of Gibraltar. Sci. Total Environ. 704, 135408 https://doi.org/10.1016/j.scitotenv.2019.135408.

Guo, Q., Majeed, S., Xu, R., Zhang, K., Kakade, A., Kahn, A., Hafeez, H.Y., Mao, C., Liu, P., Li, X., 2019. Heavy metals interact with the microbial community and affect biogas production in anaerobic digestion: a review. J. Environ. Manag. 240, 266–272. https://doi.org/10.1016/j.jenvman.2019.03.104.

Hassaan, M.A., El Nemr, A., Elkatory, M.R., Eleryan, A., Ragab, S., El Sikaily, A., Pantaleo, A., 2021. Enhancement of biogas production from macroalgae Ulva lactuca via ozonation pretreatment. Energies 14, 1703. https://doi.org/10.3390/en14061703.

Holliger, C., Alves, M., Andrade, D., Angelidaki, I., Astals, S., Baier, U., Bougrier, C., Buffière, P., Carballa, M., de Wilde, V., Ebertseder, F., Fernández, B., Ficara, E., Fotidis, I., Frigon, J.C., de Laclos, H.F., Ghasimi, D.S.M., Hack, G., Hartel, M., Heerenklage, J., Horvath, I.S., Jenicek, P., Koch, K., Krautwald, J., Lizasoain, J., Liu, J., Mosberger, L., Nistor, M., Oechsner, H., Oliveira, J.V., Paterson, M., Pauss, A., Pommier, S., Porqueddu, I., Raposo, F., Ribeiro, T., Pfund, F.R., Strömberg, S., Torrijos, M., van Eekert, M., van Lier, J., Wedwitschka, H., Wierinck, I., 2016. Towards a standardization of biomethane potential tests. Water Sci. Technol. 74, 2515–2522. https://doi.org/10.2166/wst.2016.336.

Jard, G., Marfaing, H., Carrère, H., Delgenes, J.P., Steyer, J.P., Dumas, C., 2013. French Brittany macroalgae screening: Composition and methane potential for potential alternative sources of energy and products. Bioresour. Technol. 144, 492–498. https://doi.org/10.1016/j.biortech.2013.06.114.

Jeong, H., Ra, K., 2022. Seagrass and green macroalgae halimeda as biomonitoring tools for metal contamination in Chuuk, Micronesia: pollution assessment and bioaccumulation. Mar. Pollut. Bull. 178, 113625 https://doi.org/10.1016/j.marpolbul.2022.113625.

Júnior, O.N., Dip, M.R., Góes, R.M., 1991. Macroalgae of a stream in southeastern Brazil: composition, seasonal variation and relation to physical and chemical variables. Hydrobiologia 213, 241–250. https://doi.org/10.1007/BF00016425.

Leong, Y.K., Chang, J.S., 2022. Integrated role of algae in the closed-loop circular economy of anaerobic digestion. Bioresour. Technol. 360, 127618 https://doi.org/10.1016/j.biortech.2022.127618.

Lin, R., Deng, C., Ding, L., Bose, A., Murphy, J.D., 2019. Improving gaseous biofuel production from seaweed Saccharina latissima: the effect of hydrothermal pretreatment on energy efficiency. Energy Convers. Manag. 196, 1385–1394. https://doi.org/10.1016/j.enconman.2019.06.044.

Madl, P., Yip-Wong, M., 2005. National management plan for the genus caulerpa: literature review of the aquarium strain of Caulerpa taxifolia. Aquatic Nuisance Species Control 87–135.

Magnusson, T., Zanatta, H., Larsson, M., Kanda, W., Hjelm, O., 2022. Circular economy, varieties of capitalism and technology diffusion: anaerobic digestion in Sweden and Paraná. J. Clean. Prod. 335, 130300. https://doi.org/10.1016/j.jclepro.2021.130300.

Membere, E., Sallis, P., 2018. Effect of temperature on kinetics of biogas production from macroalgae. Bioresour. Technol. 263, 410–417. https://doi.org/10.1016/j.biortech.2018.05.023.

Mercado, J.M., Gómez-Jakobsen, F., Korbee, N., Aviles, A., Bonomi-Barufi, J., Muñoz, M., Reul, A., Figueroa, F.L., 2022. Analyzing environmental factors that favour the growth of the invasive brown macroalgae rugulopteryx okamurae (Ochrophyta): the probable role of the nutrient excess. Mar. Pollut. Bull. 174, 113315 https://doi.org/10.1016/j.marpolbul.2021.113315.

Mhatre, Ap, Gore, S., Mhatre, Ak, Trivedi, N., Sharma, M., Pandit, R., Anil, A., Lali, A., 2019. Effect of multiple product extractions on bio-methane potential of marine macrophytic green alga Ulva lactuca. Renew. Energy 132, 742–751. https://doi.org/10.1016/j.renene.2018.08.012.

Michalak, I., Wilk, R., Chojnacka, K., 2017. Bioconversion of Baltic seaweeds into organic compost. Waste Biomass Valor. 8, 1885–1895. https://doi.org/10.1007/s12649-016-9738-3.

Miteco, 2022. Estrategia de control del alga rugulopteryx okamurae en España. https://www.miteco.gob.es/es/biodiversidad/publicaciones/pbl_fauna_flora_estrategia_R_okamurae.aspx accessed 8th September 2022.

Monlau, F., Sambusiti, C., Ficara, E., Aboulkas, A., Barakat, A., Carrère, H., 2015. New opportunities for agricultural digestate valorization: current situation and perspectives. Energy Environ. Sci. 8, 2600–2621. https://doi.org/10.1039/C5EE01633A.

Montingelli, M.E., Benyounis, K.Y., Quilty, B., Stokes, J., Olabi, A.G., 2016. Optimisation of biogas production from the macroalgae Laminaria sp. at different periods of harvesting in Ireland. Appl. Energy 177, 671–682. https://doi.org/10.1016/j.apenergy.2016.05.150.

Nielsen, B.V., Maneein, S., Al-Farid, M.M., Milledge, J.J., 2020. The effects of halogenated compounds on the anaerobic digestion of macroalgae. Fermentation 6, 85. https://doi.org/10.3390/fermentation6030085.

Nielfa, A., Cano, R., Fdz-Polanco, M., 2015. Theoretical methane production generated by the co-digestion of organic fraction municipal solid waste and biological sludge. Biotechnol. Rep. 5, 14–21. https://doi.org/10.1016/j.btre.2014.10.005.

Nkemka, V.N., Murto, M., 2010. Evaluation of biogas production from seaweed in batch tests and in UASB reactors combined with the removal of heavy metals. J. Environ. Manag. 91 (7), 1573–1579. https://doi.org/10.1016/j.jenvman.2010.03.004.

Olivera, J.V., Alves, M.M., Costa, J.C., 2014. Design of experiments to assess pre-treatment and co-digestion strategies that optimize biogas production from macroalgae gracilaria vermiculophylla. Bioresour. Technol. 162, 323–330. https://doi.org/10.1016/j.biortech.2014.03.155.

Paul, S., Dutta, A., 2018. Challenges and opportunities of lignocellulosic biomass for anaerobic digestion. Resour. Conserv. Recycl. 130, 164–174. https://doi.org/10.1016/j.resconrec.2017.12.005.

Paulo, L.M., Ramiro-García, J., van Mourik, S., Stams, A.J.M., Sousa, D.Z., 2017. Effect of nickel and cobalt on methanogenic enrichment cultures and role of biogenic sulphide in metal toxicity attenuation. Front. Microbiol. 8, 1341. https://doi.org/10.3389/fmicb.2017.01341.

Pardilhó, S., Cotas, J., Pereira, L., Oliveira, M.B., Dias, J.M., 2022. Marine macroalgae in a circular economy context: a comprehensive analysis focused on residual biomass. Biotechnol. Adv. 60, 107987 https://doi.org/10.1016/j.biotechadv.2022.107987.

Puri, M., Gupta, A., McKinnon, R.A., Abraham, R.E., 2022. Marine bioactives: from energy to nutrition. Trends Biotechnol. 40 (3), 271–280. https://doi.org/10.1016/j.tibtech.2021.08.004.

Rakib, M.R.J., Jolly, Y.N., Dioses-Salinas, D.C., Pizarro-Ortega, C.I., De-la-Torre, G.E., Khandaker, M.U., Alsubaie, A., Almalki, A.S.A., Bradley, D.A., 2021. Macroalgae in biomonitoring of metal pollution in the bay of Bengal coastal waters of Cox's Bazar and surrounding areas. Sci. Rep. 11, 20999. https://10.1038/s41598-021-99750-7.

Ramírez, M., González, H., Ablanedo, N., Torres, I., 1989. Heavy metals in macroalgae of Havanás northern littoral. Cuba. Chem. Ecol. 38 (3), 307–315. https://doi.org/10.1071/MF9870307.

Raposo, F., de la Rubia, M.A., Borja, R., Alaiz, M., 2008. Assessment of a modified and optimised method for determining chemical oxygen demand of solid substrates and solutions with high suspended solid content. Talanta 76, 448–453. https://doi.org/10.1016/j.talanta.2008.03.030.

Rodriguez, C., Alaswad, A., El-Hassan, Z., Olabi, A.G., 2018. Waste paper and macroalga co-digestion effect on methane production. Energy 154, 119–125. https://doi.org/10.1016/j.energy.2018.04.115.

Rose-Benish, P.M., Mozhiarasi, V., Nagabalaji, V., Weichgrebe, D., Srinivasan, S.V., 2022. Optimization of process parameters for enhanced methane production from banana peduncle by thermal pretreatment. Biomass Convers. Biorefin. https://doi.org/10.1007/s13399-022-02917-z. In Press.

Santana, I., Félix, M., Guerrero, A., Bengoechea, C., 2022. Processing and characterization of bioplastics from the invasive seaweed rugulopteryx okamurae. Polym. 14, 355. https://doi.org/10.3390/polym14020355.

Saratale, R.G., Kumar, G., Banu, R., Xia, A., Periyasamy, S., Dattatraya Saratale, G., 2018. A critical review on anaerobic digestion of microalgae and macroalgae and co-digestion of biomass for enhanced methane generation. Bioresour. Technol. 262, 319–332. https://doi.org/10.1016/j.biortech.2018.03.030.

Saveyn, H., Eder, P., 2014. End-of-waste criteria for biodegradable waste subjected to biological treatment (compost & digestate): Technical Report by the Joint Research Centre of the European Comission. http://op.europa.eu/en/publication-detail/-/publication/66031c1b-b894-4da3-b091-4e094e83f885/language-en.

Silva, J.A., Braga, A.F.M., Fermoso, F.G., Zaiat, M., Silva, G.H.R., 2021. Evaluation of the influence of trace metals on methane production from domestic sewage, using the plackett-burman experimental design. J. Environ. Manag. 294, 113002 https://doi.org/10.1016/j.jenvman.2021.113002.

Stürmer, B., Pfundtner, E., Kirchmeyr, F., Uschnig, S., 2020. Legal requirements for digestate as fertilizer in Austria and the European Union compared to actual technical parameters. J. Environ. Manage. 253, 109756 https://doi.org/10.1016/j.jenvman.2019.109756.

Suwati, S., Romansyah, E., Syarifudin, S., Jani, Y., Purnomo, A.H., Damat, D., Yandri, E., 2021. Comparison between natural and cabinet drying on weight loss of seaweed Euchuema cottonii Weber-van Bosse, 37, 1–8. https://doi.org/10.17582/journal.sja/2021/37.s1.01.08.

Thompson, T.M., Young, B.R., Baroutian, S., 2019. Advances in the pretreatment of brown macroalgae for biogas production. Fuel Process. Technol. 195, 106151 https://doi.org/10.1016/j.fuproc.2019.106151.

USEPA, 2007. Method 3051A (SW-846): Microwave Assisted Acid Digestion of Sediments, Sludges, and Oils, Revision 1. U.S. EPA, Washington, DC.

USGS, 2022. Science for a changing world. Zeolites (usgs.gov). In: U.S. Geological Service. (Accessed 9 August 2022).

Wang, X., Duan, X., Chen, J., Fang, K., Feng, L., Yan, Y., 2016. Enhancing anaerobic digestion of waste activated sludge by pretreatment: effect of volatile to total solids. Environ. Technol. 37 (12), 1520–1529. https://doi.org/10.1080/09593330.2015.1120783.

Williams, S.L., Schroeder, S.L., 2004. Eradication of the invasive seaweed Caulerpa taxifolia by chlorine bleach. Mar. Ecol. Prog. Ser. 272, 69–76. https://doi.org/10.3354/meps272069.

Yenigün, O., Demirel, B., 2013. Ammonia inhibition in anaerobic digestion: a review. Process Biochem. 48 (5–6), 901–911. https://doi.org/10.1016/j.procbio.2013.04.012.

Zheng, X., Zou, D., Wu, Q., Wang, H., Li, S., Liu, F., Xiao, Z., 2022. Review on fate and bioavailability of heavy metals during anaerobic digestion and composting of animal manure. Waste Manag. 150, 75–89. https://doi.org/10.1016/j.wasman.2022.06.033.

Zollmann, M., Robin, A., Prabhu, M., Polikovsky, M., Gillis, A., Greiserman, S., Golberg, A., 2019. Green technology in green macroalgal biorefineries. Phycologia 58 (5), 516–534. https://doi.org/10.1016/j.biotechadv.2022.107987.